Published in *Appl. Nonlin. Dynam.* **11**, 38-44 (2003).

Fluctuational transitions across locally-disconnected and locally-connected fractal basin boundaries

A. N. Silchenko, S. Beri, D. G. Luchinsky and P. V. E. McClintock
Department of Physics, Lancaster University, Lancaster, LA1 4YB, UK

August 1, 2003

Abstract

We study fluctuational transitions in a discrete dynamical system that has two co-existing attractors in phase space, separated by a fractal basin boundary which may be either locally-disconnected or locally-connected. It is shown that, in each case, transitions occur via an accessible point on the boundary. The complicated structure of paths inside the locally-disconnected fractal boundary is determined by a hierarchy of homoclinic original saddles. The most probable escape path from a regular attractor to the fractal boundary is found for the each type of boundary using both statistical analyses of fluctuational trajectories and the Hamiltonian theory of fluctuations.

1 Introduction

The stability of nonlinear multistable systems in the presence of noise is of great importance for practical applications [1, 2]. It is well known that nonlinear dynamical systems can demonstrate sensitivity to initial conditions, even in the absence of limit sets with complex geometrical structure in their phase space. The reason lies in the complex structure of the basins of attraction, which may be fractal [3, 4, 5, 6, 7, 8], thus raising some challenging and difficult problems. For example, how does a fluctuational transition take place across a fractal basin boundary (FBB)? What is the difference, if any, in the transition mechanism for the different types of FBB? If transitions across FBBs are characterised by general features, a knowledge of them could considerably simplify investigations of stability and control for chaotic dynamical systems, both of which are topical problems of broad interdisciplinary interest [9, 10, 11].

A promising approach to this problem is based on the analysis of fluctuations in the limit of small noise intensity: the system fluctuates to remote states along most probable deterministic paths [12, 13, 14] that correspond to rays in the WKB-like asymptotic solution of the Fokker-Planck equation [15]. The approach has been extended to chaotic systems, both continuous and discrete, [16, 17, 18, 19]. It was shown recently that the homoclinic tangencies responsible for fractalization of the basins cause a decrease in the activation energy [20]. However, there are still no theoretical predictions about the mechanism of escape in the case of an FBB. Unsolved problems include the uniqueness of the escape path, the form of the boundary conditions on the FBB and, as already mentioned,whether or not the mechanism of escape depends on the type of FBB under consideration.

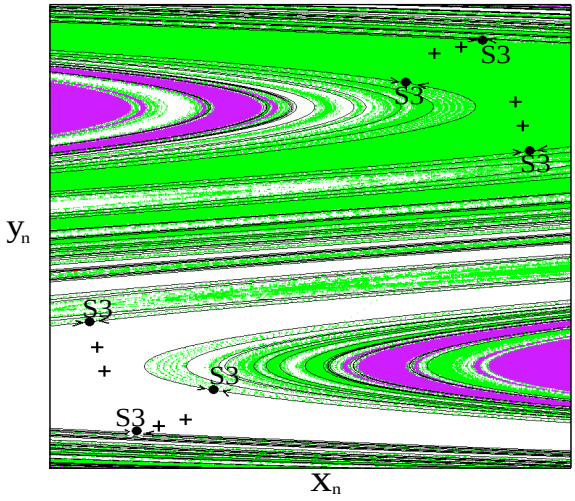

Figure 1: The co-existing stable points of period 4 (black crosses) and their basins of attraction, shown in grey and white respectively. The accessible boundary saddle points of period 3 are indicated by the small filled circles S3. Their stable manifolds are drawn as solid black lines.

In this paper, we describe the mechanisms of fluctuational transition for two different types of FBB, namely, locally-disconnected (LD) and locally-connected (LC) FBBs. We show below that in spite of the large qualitative differences between these types of FBB, their mechanisms of fluctuational transition are characterised by a universal common feature.

2 Transitions across a locally-disconnected FBB

There are known to be several types of FBB in different dynamical systems [4, 6, 7, 8]. The LD FBB represents the simplest and commonest, and it is the only type of FBB to have been observed in experiments [4, 5]. As we will show below, the mechanism of fluctuational transition across it is determined primarily by its deterministic structure, which enables us to infer that the mechanism must be generic to all systems with FBBs of this kind. To reveal the transition mechanism across an LD FBB, we take as our model the two-dimensional map introduced by Holmes [21]

$$\begin{aligned} x_{n+1} &= f_1(x_n, y_n) = y_n \\ y_{n+1} &= f_2(x_n, y_n, \xi_n) = -b\,x_n + d\,y_n - y_n^3 + \xi_n, \end{aligned} \tag{1}$$

where ξ_n is white Gaussian noise with $\langle\, \xi_n \,\rangle = 0$, and $\langle \xi_n \xi_m \rangle = 2D\,\delta_{nm}$. In what follows we will adopt the notation $\mathbf{x_n} = \{x_n, y_n\}$, $\mathbf{f} = \{f_1, f_2\}$ and $\xi_\mathbf{n} = \{0, \xi_n\}$. Due to symmetry, the system (1) has pairs of co-existing attractors for $b = 0.2$ and $2.0 \leq d \leq 2.745$. Their basins are separated by a boundary that may be either smooth or fractal depending on the chosen parameter values. We choose for our studies $b = 0.2$ and $d = 2.65$, which corresponds to there being two co-existing stable points of period 4 whose basins are separated by an LD FBB (see Fig. 1). The fractal dimension of the boundary is equal to 1.8451.

To find the boundary conditions on the LD FBB, and the optimal fluctuational force steering the system (1) from one co-existing attractor to another, we will make use of an analogy between energy-optimal control and noise-induced escape from a basin of

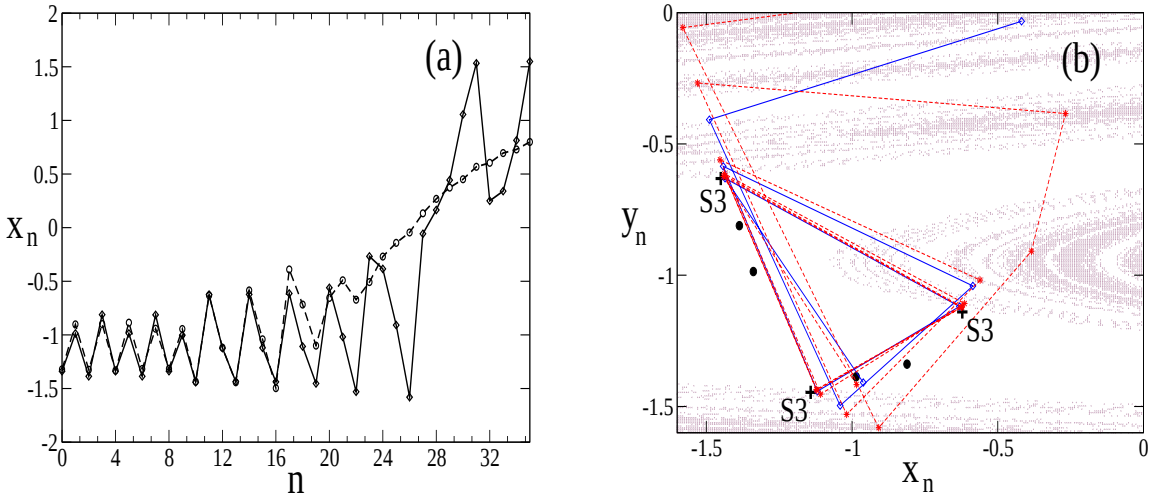

Figure 2: (a) The most probable escape path (dashed line) connecting the stable point of period 4 with the period-3 saddle cycle lying on the fractal boundary obtained from the numerical simulations with $D = 10^{-5}$. The optimal path found by the solution of the boundary-value problem is shown as a solid line; (b) a two-dimensional plot of the paths presented in the previous figure.

attraction. We have modelled (1) numerically, exciting the system with weak noise and collecting both the escape trajectories between the attractors and also the corresponding noise realisations inducing the transitions. By ensemble-averaging a few hundred such escape trajectories and noise realisations, we have obtained the optimal escape path (see Fig.2) and corresponding optimal force shown in Fig. 3. In the case of the LD FBB, these results allow us both to determine the boundary conditions near the boundary, and to demonstrate the uniqueness of the most probable escape path (MPEP). A typical optimal escape path is shown in Fig. 2(a). A simple analysis of the optimal path shows that the system (1) leaves the stable point of period 4 and moves to the LD FBB, crossing it at a point of period 3 located near, or directly on, the LD FBB (see Fig. 2(a)). Simple calculations have shown that a saddle point of period 3, S3, in Fig. 1 and Fig. 2(b) with multipliers $\rho_1 = 0.001218$ and $\rho_2 = 6.566269$) does exist for the chosen parameter values and that it lies on the boundary. Moreover, its stable manifold (solid black line in Fig. 1) is dense in the boundary and detaches the open neighborhood including the attractor from the LD FBB itself, allowing us to classify it as an accessible boundary point [22]. It is well known that the energy-optimal path is given by that path which minimises the sum $\mathbf{S} = 1/2 \sum_{\mathbf{n=1}}^{\mathbf{N}} \xi_{\mathbf{n}}^{\mathbf{2}}$, where $\xi_{\mathbf{n}}$ is the noise realization moving the system from one attractor to the other. The extremal problem can easily be solved by taking (1) into account by means of Lagrangian multipliers $\lambda_{\mathbf{n}}$ [18], yielding the following Lagrangian for minimization:

$$\mathbf{L} = \frac{1}{2} \sum_{\mathbf{n=1}}^{\mathbf{N}} \xi_{\mathbf{n}}^{\mathbf{T}} \, \xi_{\mathbf{n}} + \sum_{\mathbf{n=1}}^{\mathbf{N}} \lambda_{\mathbf{n}}^{\mathbf{T}} \, (\mathbf{x_{n+1}} - \mathbf{f}(\mathbf{x_n}) - \xi_{\mathbf{n}}),$$

where $\mathbf{x_{n+1}}$, $\mathbf{f}(\mathbf{x_n})$ and $\xi_{\mathbf{n}}$ are the two-dimensional vectors defined in (1). Further, varying $\mathbf{L}$ with respect to $\xi_{\mathbf{n}}$ and $\mathbf{x_n}$ we get the following two-dimensional map:

$$\begin{aligned} x_{n+1} &= y_n \\ y_{n+1} &= -b\, x_n + d\, y_n - y_n^3 + \lambda_n^y \\ \lambda_{n+1}^x &= (d - 3x_{n+1}^2)\, \lambda_n^x / b - \lambda_n^y / b \\ \lambda_{n+1}^y &= \lambda_n^x \end{aligned} \qquad (2)$$

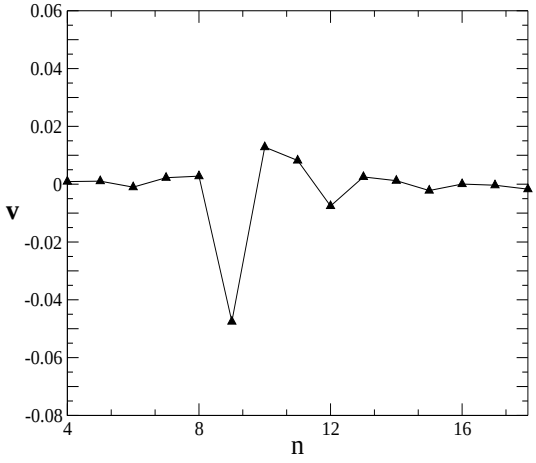

Figure 3: The optimal fluctuational force obtained from the Monte-Carlo simulations.

Equations (2) are supplemented by the following boundary conditions

$$\lim_{\mathbf{n}\to-\infty} \lambda_{\mathbf{n}} = \mathbf{0}, \;\; \mathbf{x_n^0} \in \mathbf{attractor}, \;\; \mathbf{x_n^1} \in \mathbf{LD\,FBB}. \tag{3}$$

In fact, the unique energy-optimal trajectory along which $\mathbf{S}$ takes its minimal value is a heteroclinic trajectory in the four-dimensional phase space of the system (2), connecting the stable point of period 4 with a point on the boundary. At this stage, we are ready to solve the corresponding boundary-value problem for (2) numerically. This can be done via a procedure involving shooting from a very small neighbourhood of the chosen saddle point, parameterizing the initial conditions as points lying on a two-dimensional unstable manifold of this saddle point, characterized by the appropriate radius r and angle ϕ, and with subsequent selection of the trajectory minimizing S. Initial values for the coordinates can be parameterised by the distance from the initial state and angular position; the initial values for the λ_n are obtained by using the equations for the linearised manifold. During the evolution of the system (2) far from its initial state, we collect the values $\mathbf{S_{n+1}} = \mathbf{S_n} + \mathbf{1/2}\,\lambda_{\mathbf{n}}^{\mathbf{T}}\,\lambda_{\mathbf{n}}$ and plot $\mathbf{S_n}$ as a function of the two parameters. Thus, the global minimum of the activation energy gives us the parameters corresponding to the optimal escape path. We emphasise that the optimal trajectory is physically real, and not just a mathematical abstraction. In fact, when the system (1) is driven by noise whose intensity tends to zero, the escape events become exponentially rare, but they take place in an almost deterministic way following very closely the deterministic trajectory of (2). As clearly seen from Fig. 2, the phase trajectory in (2) along which S takes its minimal value coincides with the MPEP obtained by taking an ensemble average of successful trajectories. Note that no action is required to bring the system to the other attractor after it has hit the FBB, and neither is there any possibility of controlling the motion inside the LD FBB.

Analysis of the structure of escape paths inside the LD FBB has shown that homoclinic saddle points play a key role. In the system (1), we observe an infinite sequence of saddle-node bifurcations of period $3, 4, 5, 6...$, occurring at parameter values $d_3 < d_4 < d_5 < d_6...$ and caused by sequential tangencies of the stable and unstable manifolds of the saddle point O at (0, 0). The homoclinic orbits appearing as the result of these bifurcations were classified earlier as *original saddles*, and it was also shown that their stable and unstable manifolds cross each other in hierarchical sequence [22]. To characterize this hierarchical relationship between original saddles it is reasonable to use the ratio

$$\mu = \mid \lambda_{st}(S) \mid / \lambda_{un}(S)$$

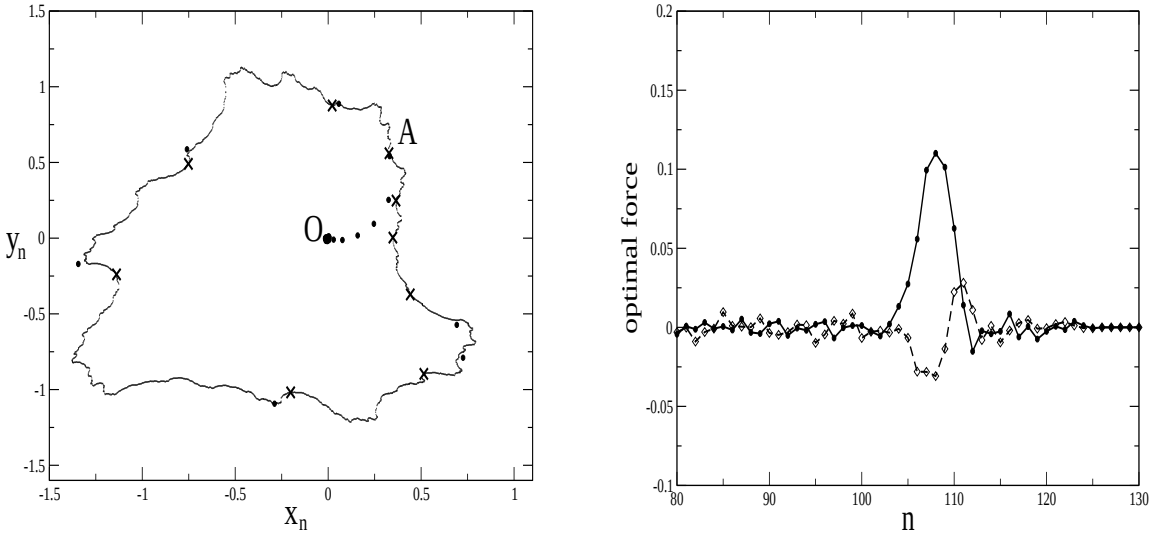

Figure 4: Left: the locally-connected FBB (solid closed curve), unstable node of period 9 (crosses) and points of the optimal escape path obtained from the Monte-Carlo simulations (filled circles) with $D = 5 \cdot 10^{-3}$. Right: x (solid line) and y (dashed line) components of the optimal fluctuational force.

where $\lambda_{st}(S)$ and $\lambda_{un}(S)$ are the stable and unstable eigenvalues of the Jacobian matrix of (1) at the saddle point S. Simple calculations have shown that, for the original saddles of period $3, 4, 5, 6...$ in (1), the following hierarchical sequence of index μ values occurs: $\mu_3 = 3.566$, $\mu_4 = 3.301$, $\mu_5 = 3.249$, $\mu_6 = 3.142$. It is known that unstable periodic orbits embedded within a chaotic saddle define a distribution of the natural measure on it both for hyperbolic and nonhyperbolic dynamical systems [23, 24]. In particular, the natural measure η on a two-dimensional chaotic non-attracting set is concentrated along its unstable manifold and can be represented via unstable eigenvalues of unstable orbits: $\eta(C) = \sum 1/\lambda^{un}(x_i)$, where C is the region of phase space containing the chaotic saddle, $\lambda^{un}(x_i)$ is the eigenvalue corresponding to the unstable manifold and the summation is over all the unstable orbits x_i in C [24] (cf. [23]). A statistical analysis of escape trajectories has shown that these probabilities demonstrate a hierarchical interrelation [25], which is in a good agreement with the distribution of the natural measure on the chaotic saddle O forming the LD FBB.

3 Transitions across a locally-connected FBB

We now consider the same escape problem, but in a system possessing an LC FBB. This type of FBB is generally observed in two-dimensional noninvertible analytic and nonanalytic maps [4, 26]. We take as our model a typical quadratic conformal map:

$$\begin{aligned} x_{n+1} &= x_n^2 - y_n^2 + 0.7\,x_n + \xi_n^1 \\ y_{n+1} &= 2\,x_n y_n + 0.7\,x_n + 0.5\,y_n + \xi_n^2 \end{aligned} \tag{4}$$

where ξ_n^1, ξ_n^2 are statistically independent sources of white, Gaussian, noise of zero mean that are of the same intensity D as each other. This map has stable points at the origin and at infinity, separated by the LC FBB. The boundary contains an infinite set of repelling points and, in this case, no stable or saddle points. Note that noise-induced escape from the attractor surrounded by the LC FBB in (4) was considered earlier in the pioneering work of Grassberger [18], who succeeded in calculating the optimal escape path, albeit without finding the boundary condition on the LC FBB or the mechanism of escape.

To find the boundary condition on the LC FBB and the optimal escape path, we use exactly the same technique as in the case of the LD FBB, above. The results of our calculations are presented in Fig. 4. As clearly seen from this figure, the system (4) leaves the stable point O at the origin along the unique optimal escape path and approaches the LC FBB at the unique point shown in Fig. 4 (left). Moreover, our calculations have shown that the optimal fluctuational force (see Fig. 4 (right)) becomes equal to zero at this moment. According to our previous results, this means that the system (4) reached the boundary at this point, and its further relaxation to infinity is noise-free and completely specified by the deterministic structure of the FBB. Our calculations have shown that the boundary point A corresponds exactly to the repelling boundary point of period 9, which plays the role of the unique boundary condition on this LC FBB. These results were further confirmed by numerical solution of the boundary-value problem for the corresponding four-dimensional extended map. To approach an understanding of why this repelling point should play the role of the boundary condition, it is necessary to look more closely at the structure of the LC FBB, which is the Julia set $J(\mathbf{x})$. It is well known that the Julia set contains a dense set of repelling points [27]. However, these points are not all the same, and they may be classified in terms of their local instability. Indeed, there are two types of repelling points forming the LC FBB in (4), namely, unstable nodes and unstable focuses. Every unstable node on the LC FBB has a part of its unstable manifold connecting it to the stable point O and lying fully inside its basin of attraction, whereas this is not true of a focus. By definition, a point $\mathbf{x}$ is accessible if there is a continuous curve $\gamma : [0, \infty) \to C$ for which $\gamma(n)$ lies in the basin of attraction of $\mathbf{x}$ for all n and $\lim_{n\to\infty} \gamma(n) = \mathbf{x}$. This fact enable us to conclude that unstable nodes form a countable set of accessible points on the LC FBB. The presence of a countable set of accessible points was rigorously proven [28] quite recently. Our calculations have shown that accessible boundary points are distributed nonuniformly on the boundary, and that their multipliers, have different values which, in turn, may lead to a hierarchal interrelationship between them. The quest for such a hierarchy, and further generalizations of our approach presented above, represent goals of our future investigations.

4 Conclusions

In conclusion, we have studied fluctuational transitions between co-existing regular attractors separated by both the LD and LC FBB. We have shown that an accessible point on the FBB plays the role of a unique boundary condition for both types of FBB. Our statistical analyses of fluctuational trajectories have yielded solutions of the boundary-value problem for both types of FBB, and have revealed the optimal fluctuational forces moving the systems (1) and (4) from one attractor to the other. We were also able to find the unique optimal escape path in both cases. The original saddles forming the homoclinic structure of the system (1) play a key role in the formation of the escape paths inside the LD FBB, and the difference in their local stability defines the hierarchical relationship between them. The results obtained can be applied directly to the other maps and flows having the same type of FBB.

Acknowledgements

The research has been supported by the Engineering and Physical Sciences Research Council (UK) and INTAS.

References

[1] *Stratonovich R. L* Topics in the Theory of Random Noise (Mathematics and its Applications) // Taylor and Francis, 1967.

[2] *Anishchenko V. S., Neiman A.B., Vadivasova T. E., Schimansky-Geier L., Astakhov V. V.* Nonlinear dynamics of Chaotic and Stochastic Systems // Springer Verlag, 2001.

[3] *Ott E.,* Chaos in Dynamical Systems //Cambridge University Press, 2002.

[4] *McDonald S. W, Grebogi C., Ott E., and Yorke J. A.,* Fractal basin boundaries // Physica, 1985, VOL. 17D, P. 125.

[5] *Cartwright M. L. and Littlewood J. E.,* //Ann. Math. 1951, VOL. 54, P. 1; *Moon F. C. and Li G. -X.,* //Phys. Rev. Lett. 1985, VOL. 55, P. 1439.

[6] *Sommerer J. C., and Ott E.,* A physical system with qualitatively uncertain dynamics //Nature, 1993, VOL. 365, P. 135;

[7] *Nusse H. E., and Yorke J. A.,* Basins of attraction //Science, 1996, VOL. 271, P. 1376;

[8] *Hunt B. R., Ott E., Rosa E.,* Sporadically fractal basin boundaries of chaotic systems //Phys. Rev. Lett. 1999, VOL. 82, 3597.

[9] *Fradkov A. L. and Pogromsky A. Y.*, Introduction to Control of Oscillations and Chaos // Series on Nonlinear Science A, vol. 35 World Scientific, Singapore, 1998.

[10] *Boccaletti S., Grebogi C., Lai Y. C, Mancini H., Maza D.* The control of chaos: theory and applications //Phys. Rep, 2000 VOL. 39, P. 103.

[11] *Shinbrot T., Grebogi C., Ott E. and Yorke J. A.,* Using small perturbations to control chaos //Nature (London), 1993, VOL. 363, P. 411; *Auerbach D., Grebogi C., Ott E. and Yorke J. A,* Controlling Chaos in High Dimensional Systems //Phys. Rev. Lett., 1992, VOL. 69, P. 3479.

[12] *Onsager L., and Machlup S.,* Fluctuations and irreversible processes //Phys. Rev., 1953, VOL. 91, P. 1505.

[13] *Dykman M. I., McClintock P. V. E., Smelyanskiy V. N., Stein N. D., and Stocks N. G.,* Optimal paths and the prehistory problem for large fluctuations in noise driven systems //Phys. Rev. Lett., 1992, VOL. 68 P. 2718.

[14] *Luchinsky D. G., Maier R. S., Mannella R., McClintock P.V.E., Stein D. L.,* Experiments on critical phenomena in a noisy exit problem //Phys. Rev. Lett., 1997, VOL. 79, P. 3117; *Luchinsky D. G.,* On the nature of large fluctuations in equilibrium systems: observation of an optimal force //J. Phys. A, 1997, VOL. 30, P. L577; *Luchinsky D. G. and McClintock P. V. E.,* Irreversibility of classical fluctuations studied in analogue electrical circuits //Nature, 1997, VOL. 389, P. 463.

[15] *Freidlin M. I. and Wentzel A. D.,* Random Perturbations in Dynamical Systems //Springer, New York, 1984.

[16] *Kautz R. L.,* Activation energy for thermally induced escape from a basin of attraction //Phys. Lett. A, 1987 VOL. 125, P. 315.

[17] *Beale P. D.,* Noise-induced escape from attractor in one-dimensional maps //Phys. Rev. A, 1989 VOL. 40, P. 3998.

[18] *Grassberger P.,* Noise-induced escape from attractors //J. Phys. A: Math. Gen., 1989 VOL. 22, P. 3283.

[19] *Graham R., Hamm A., and Tel T.,* Nonequilibrium potentials for dynamical systems with fractal attractors or repellers //Phys. Rev. Lett., 1991 VOL. 66, P. 3089.

[20] *Soskin S. M., Arrayás M., Mannella R., and Silchenko A. N.,* Strong enhancement of noise-induced escape by nonadiabatic periodic driving due to transient chaos//Phys. Rev. E., 2001, VOL. 63, P. 051111.

[21] *Holmes P.,* A nonlinear oscillator with a strange attractor //Phil. Trans. R. Soc., 1979, VOL. A292, P. 419.

[22] *Grebogi C., Ott E., and Yorke J. A.,* Basin boundaries metamorphoses - changes in accessible boundary orbits //Physica, 1987, VOL. 24D, P. 243.

[23] *Grebogi C., Ott E., and Yorke J. A.,* Unstable periodic orbits and the dimensions of multifractal chaotic attractors, //Phys. Rev. A, 1988, VOL. 37, P. 1711.

[24] *Dhamala M. and Lai Y.-C.,* The natural measure of nonattracting chaotic sets and its representation by unstable periodic orbits //Int. J. Bif. Chaos, 2002, VOL. 12, P. 2991.

[25] *Silchenko A. N., Luchinsky D. G., and McClintock P. V. E.,* Noise-induced escape through a fractal basin boundaries //Physica A, to be published.

[26] *Gardini L., Mira C., Barugola J., Cathala J. C.* Chaotic Dynamics in Two-Dimensional Noninvertible Maps //World Scientific Publishing, 1996.

[27] *Devanye R. L.* Intoduction to Chaotic Dynamical Systems //Addison-Wesley, New-York, 1989.

[28] *Bhattacharjee R, and Devaney R. L.* Tying hairs for the structurally stable exponentials //Ergodic Theory and Dynamical Systems, 2000, VOL. 20 P. 1603.